MOLEKUL
eISSN: 2503-0310

Articles
https://doi.org/10.20884/1.jm.2023.18.1.5510

Adsorption of Rhodamine B on Spherical Activated Carbon synthesized from Waste Bagasse Liquid using Hydrothermal Process

Uyi Sulaeman*, Baynuri Ikhya Ulumuddin, Roy Andreas, Irmanto Irmanto, Ponco Iswanto

Department of Chemistry, Jenderal Soedirman University, Purwokerto, 53123, Indonesia

*Corresponding author email: sulaeman@unsoed.ac.id

Received March 01, 2022; **Accepted** February 12, 2023; **Available online** March 20, 2023

ABSTRACT. The dyes of the textile dyeing industry wastewater are harmful to humans and the environment. They should be treated before discharging into the environment. The adsorption using the spherical activated carbon can be effective to reduce the dyes. The spherical activated carbon of 3-7 μm in diameter was successfully prepared from the waste bagasse liquid using the hydrothermal method. The activation of this carbon was carried out using the KOH solution. The optimum pH and contact time were achieved in 2 and 200 min, respectively. Adsorption kinetic for RhB on activated spherical carbon follows the second-order kinetics and its adsorption mechanism follows the Langmuir isotherm. The maximum adsorption capacity of spherical activated carbon to Rhodamine B was achieved in 64.52 mg/g.

Keywords: adsorption, Elovic, Freundlich, Langmuir, spherical activated carbon, Temkin.

INTRODUCTION

The technology of water treatment has played an important role in human life and the environment. It should urgently be provided due to the rapid development of industry that produced wastewater as a byproduct. The textile industry utilizes synthetic dyes as one of the process units for colouring. Dye liquid waste can be harmful to the environment and humans. Therefore, it should be treated before discharging into the environment. One method to handle this problem is adsorption using activated carbon.

Activated carbon is a very popular material and is widely used as an adsorbent due to its efficient and economical application. The activated carbon has been applied for the adsorption of hydrogen sulfide (H_2S) (Harihastuti et al., 2015), chrome metal (Cr) (Arneli et al., 2017), carbon dioxide (CO_2) (Harihastuti et al., 2017), carbon monoxide (CO) (Fikri & Veronica, 2018), surfactants (Arnelli et al., 2018), and ammonia (Ruhmawati et al., 2019). Activated carbon could be produced from coconut husk (Aljeboree et al., 2017), Acacia mangium wood (Danish et al., 2018), risk husk (Yaumi et al., 2018), and pineapple plant leaf (Beltrame et al., 2018). The adsorption in activated carbon is very closely related to its intrinsic characteristic that could be influenced by synthesis and the activation method. Therefore, the development of methods to improve the activated carbon material adsorption process is still a challenge for researchers.

Among the activated carbon, spherical activated carbons (SACs) are very interesting material due to having a large surface area (Li et al., 2016), high mechanical strength (Amorós-Pérez et al., 2018), and good thermal stability (Bedin et al., 2018). Many preparations of spherical activated carbon have been developed by researchers. Porous carbon spheres (PCSs) were successfully prepared from starch using hydrothermal and CO_2 activation (Li et al., 2016). This material can be utilized for the storage of gases such as CO_2, CH_4, and H_2. Mesoporous spherical activated carbon can be synthesized using a soluble low molecular weight phenolic resol using a sol-gel reaction under ammonium alginate (Wang et al., 2018). This modification improves the isobutane conversion and isobutene selectivity. The modifications of hydrophobic characteristics on the spherical activated carbon can be designed by polymer-based spherical activated carbon (PBSAC). This design can be utilized for hormone interaction (Tagliavini et al., 2017).

Recently, spherical carbon has been utilized as a composite material to improve its properties. The iron oxide and carbon sphere (FeO/CS) composite synthesized in a hydrothermal process was successfully applied for the photodegradation of perfluorooctanoic acid (PFOA) (Xu et al., 2020). This composite can effectively adsorb and degrade the PFOA under light irradiation. The carbon sphere (CS) can also be utilized in the composite of zeolitic imidazolate framework that can be used for oxygen

reduction reactions (Chai et al., 2020). This composite exhibited higher electrochemical stability compared to the Pt/C composite. Another composite, magnesium oxide/hollow carbon sphere (MgO/HCS) induced the adsorption and activation of CO_2 for electro-reduction (Li et al., 2020). This catalyst shows good selectivity for CO production. The unique composite adsorbent of polyaniline/nano hollow carbon sphere can also be synthesized by in-situ polymerization (Wang et al., 2021). This material can effectively adsorb the Cr(VI) and reduce it into Cr(III) which has low toxicity.

Due to widely application of spherical activated carbon in material modification, therefore preparation is very important. Herein, the spherical carbon from the waste bagasse liquid was prepared using the hydrothermal carbonization method. Based on the literature study, the preparation of spherical activated carbon from waste bagasse liquid using a hydrothermal process has not been reported by other researchers. Waste bagasse liquid from the sugar industry waste is a problem due to polluting the environment. It is very useful if these waste bagasse liquids can be processed into useful materials such as spherical activated carbon. Therefore, this experiment tried to provide a simple method of spherical activated carbon formation. The product of materials was applied to Rhodamine B (RhB) adsorption. The kinetics and isotherm adsorption were also comprehensively evaluated.

EXPERIMENTAL SECTION

Materials

The experiments used the material of waste bagasse liquid, KOH (Merck), HCl (Merck), NaOH (Merck), deionized water, ethanol (Merck), and Rhodamine B (RhB).

Spherical Activated Carbons (SACs) Synthesis

The synthesis of activated carbon was carried out using the hydrothermal carbonization method. The waste bagasse liquid was used as a precursor of carbon synthesis. An amount of 35 mL of waste bagasse liquid was introduced into the hydrothermal reactor and heated at 190 °C for 11 h. The precipitate was filtered and washed using ethanol and water. This product was dried in an oven at 105 ° C for 12 h and sieved using a 100 mesh sieve.

The activation of spherical carbon was carried out using a KOH solution. A total of 5 g of spherical carbon was mixed with 100 mL of 3 M KOH then stirred under 80 °C for 60 min with a speed of 200 rpm, and then maintained for 24 h at room temperature. The product was filtered, dried, and heated at 500 °C for 60 min. The product was washed with 1M HCl and water dried in an oven at 105 °C for 2 h. The products before and after activation were characterized using SEM (Jeol JSM-6510) and BET (Quantachrome Instruments, Nova).

The Effect of pH

The effect of pH on the adsorption was investigated using RhB adsorption. The amount of 0.2 g of spherical activated carbon was introduced into 100 mL of RhB solution (20 ppm), then stirred at 180 rpm for 4 h at room temperature. The pH variations of 1, 2, 3, 4, 5, 6, 7, 8, and 9 were prepared using 1 M HCl and 1 M H_2SO_4 for acid condition and 1 M NaOH for alkaline condition. The value of pHs was measured using a pH Meter (OHAUS, pH Meter ST3100-F).

The Effect of Contact Time

Rhodamine B solution of 20 ppm in pH optimum adsorption was introduced into a 100 mL Erlenmeyer flask and then added with 0.2 g of SACs. This solution was mixed under stirring with a speed of 180 rpm at room temperature. The time variations were set at 0, 5, 10, 20, 50, 100, 150, 200 and 240 min. The solution was filtered and the RhB concentration was determined using a UV-Vis spectrophotometer.

Adsorption Isotherm

The adsorption isotherm was carried out by varying the concentration of 100 mL RhB from 0 to 400 ppm in the Erlenmeyer flask. The activated carbon of 2.0 g was introduced into that solution and stirred at the speed of 180 rpm at room temperature. The RhB concentration was measured using a UV-Vis spectrophotometer. The isotherm adsorption models of Langmuir, Freundlich, Temkin, and Elovic on the spherical activated carbon were investigated.

RESULTS AND DISCUSSION

Spherical Activated Carbon Synthesis

The synthesis of spherical activated carbon from a waste bagasse liquid was successfully produced by the hydrothermal method. The black spherical carbon particle suspension could be successfully provided by hydrothermal. The spherical carbon exhibited a similar size of 3-7 μm in diameter before and after activation as shown in **Figure 1.**

The mechanism for spherical carbon formation was described in the previous report (Isahak et al., 2013; Sevilla & Antonio, 2009). The mechanism of spherical carbon formation generally undergoes three reaction processes including hydrolysis, dehydration, and nucleation. The hydrolysis could be induced by a hydrothermal reaction. In this reaction, the sucrose in waste bagasse liquid could be hydrolyzed into smaller compounds such as glucose and fructose. After hydrolysis, the reaction of dehydration occurs. The reaction of dehydration under the hydrothermal method occurs at a temperature of more than 180°C (Li et al., 2011). In this reaction, the ratio of H/C and O/C atoms decreases significantly and enriches the carbon content. Carbon and water can be defined as a product of dehydration reactions. The next reaction of spherical carbon formation is nucleation. Nucleation

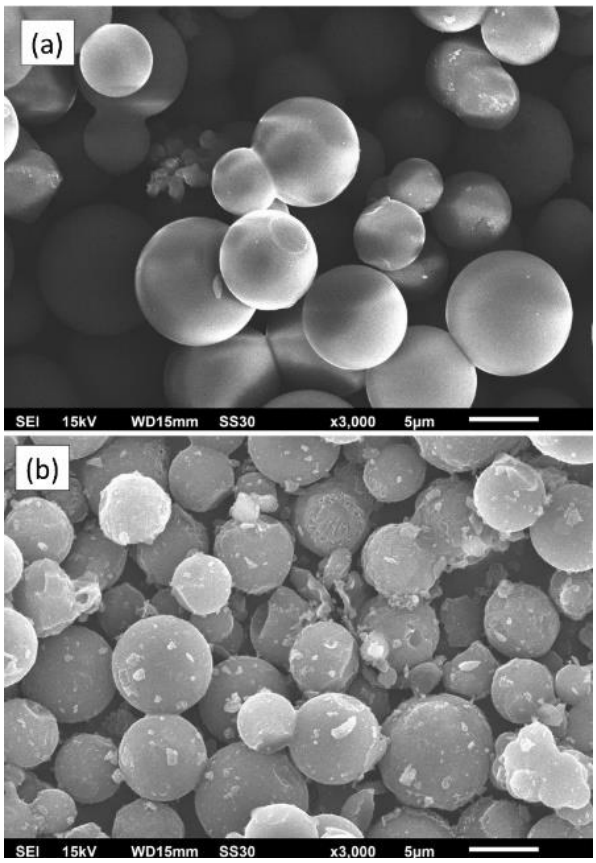

Figure 1: The spherical shape of carbon particles before activation (**a**) and after activation (**b**).

occurs when the carbon has reached a saturated concentration (Qi et al., 2016). The core of carbon particles grows iso-tropically from its surface and expanse uniformly in all directions leading to a spherical carbon formation.

The process of carbon formation, theoretically, would only form carbon and water (Guo & Lua, 2002). KOH can arrange the pore structure of activated carbon, favouring micropore formation and −OH formation leading to an increase in specific surface area and adsorption capacity (Liu et al., 2020; Sun et al., 2020). In this experiment, the KOH solution was used as an activator, and the product of spherical activated carbon was obtained.

The carbon synthesized was sieved using a 100 mesh size sieve to obtain uniform particles. At the beginning of the activation process, pre-treatment is carried out by mixing the carbon powder and KOH solution at the temperature of 80 °C. High temperatures can accelerate particle movement and increase the kinetic energy to have more collisions, therefore the KOH penetration in carbon material could be enhanced (Gad & El-Sayed, 2009). The process of immersing carbon material in KOH solution for 24 h was conducted to impregnate the KOH into each inner layer of carbon. The carbon material is then heated to 500 °C to allow the reaction of KOH and carbon (Lua & Yang, 2004). Before and after activation, the samples were characterized using SEM, and the results are shown in **Figure 1**. The spherical shape of carbon particles was observed both before and after activation. A small amount of spherical activated carbon might be broken due to carbon erosion during the KOH treatment which spread on the surface of the activated carbon as shown in **Figure 1b.**

The adsorption and desorption isotherms for N_2 are displayed in **Figure 2**. Based on the IUPAC classification scheme (Rouquerol, Rouquerol, & Sing, 1999), type III/I was observed on the sample before activation and changed into type II/IV after activation. N_2 desorption from the sample after activation showed quite a significant hysteresis, indicating that activation improves the porosity of spherical carbon. Before activation, the BET surface area, total pore volume, and average pore size showed 37.27 m^2/g, 0.0267 cc/g, and 14.31 Å, respectively. After activation, they increased to 61.06 m^2/g, 0.135 cc/g, and 44.24 Å, respectively.

Barrett–Joyner–Halenda (BJH) model is commonly used to characterize the adsorption/desorption isotherm. Based on the BJH method, the surface area of the cumulative adsorption and desorption of the un-activated sample is 13.64 m^2/g and 11.46 m^2/g, respectively, and increased significantly to 35.55 m^2/g and 100.1 m^2/g in the activated sample, respectively.

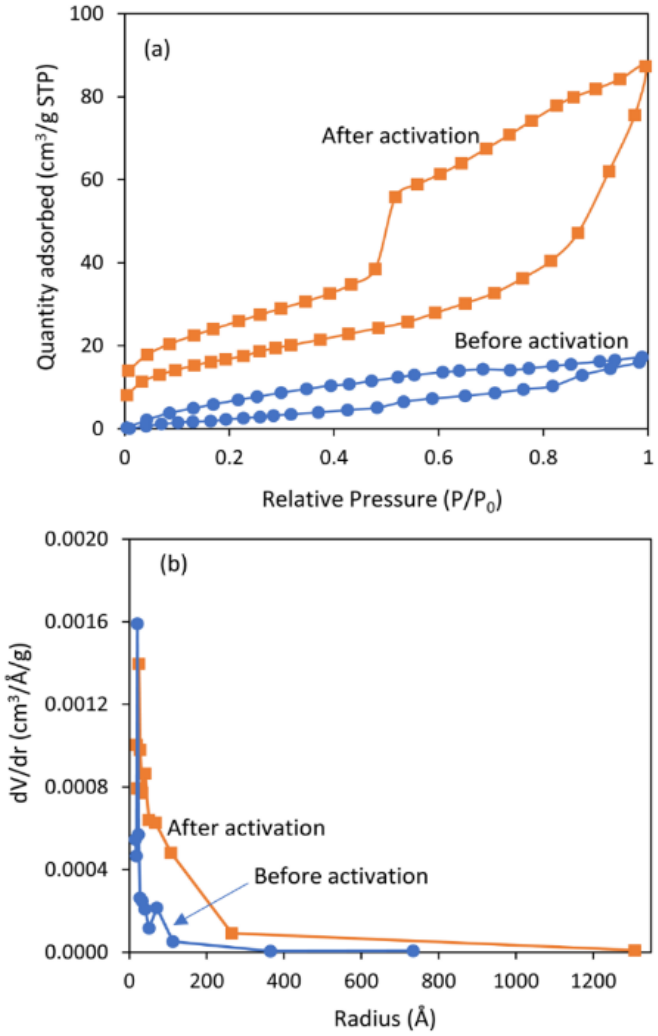

Figure 2. N_2 adsorption and desorption isotherms (**a**), pore size distribution curves of spherical carbon before and after activation (**b**).

Effect of Solution pH

The pH of the solution is one of the parameters that affect the adsorption process (Zhu et al., 2014). The pH value affects the surface of the adsorbent, ionization, and species adsorbed on the surface. **Figure 3** exhibited the adsorption of RhB under various pH conditions. The highest amount of RhB (8.126 mg/g) that adsorbed on the spherical carbon was observed at pH 2. The molecular form of RhB might be influenced by pH conditions. At acidic pH, the RhB might be stable in the cationic phase and remain in a monomeric form that makes it easier to enter into the active carbon pore (Gad & El-Sayed, 2009). The acidic environment could generate protonation of RhB and maintain the cationic phase. RhB is stable in the cationic phase under a pH lower than 4.

Rhodamine B adsorption decreases at the higher pH condition (more than pH 3) due to the formation of the RhB zwitterion phase. This phase causes enhanced aggregation and forms a larger molecule of the dimer. The dimer is a molecule composed of two monomers that are identical and bonded physically or chemically. At pH> 3.7, the RhB molecule can form the zwitterion phase (Inyinbor et al., 2015). Other researchers reported that zwitterion can be formed at conditions of pH> 3.5 (Ding et al., 2014). The higher the pH the more RhB in the dimer phase which is difficult to enter into the pores of activated carbon. The larger molecular decreases the adsorption capacity (Gad & El-Sayed, 2009).

Effect of Contact Time

Contact time is an important variable in the adsorption process. The relationship between contact time and RhB adsorbed on spherical activated carbon is presented in **Figure 4**. The longer the contact time, the more RhB could be adsorbed. The optimum contact time could be achieved when the adsorption process reached equilibrium. At the beginning of the reaction, the adsorption is higher than the desorption, resulting in the curve increasing rapidly. The equilibrium was achieved at 200 min when the rate of adsorption and desorption were equal. Therefore, the optimum contact time was achieved in 200 min, and the capacity of RhB adsorption was 8.965 mg/g.

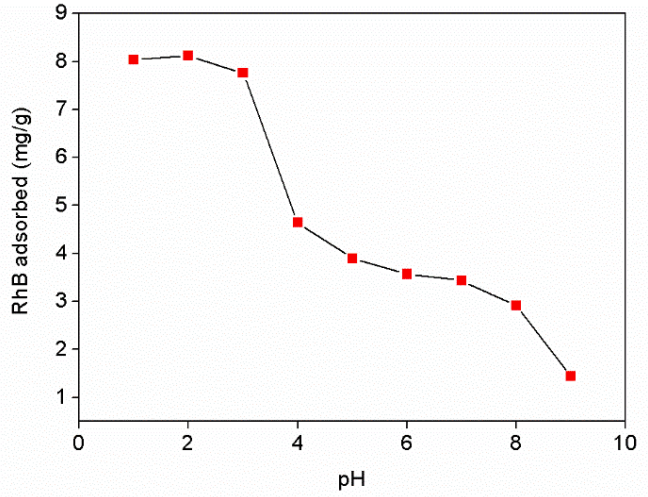

Figure 3. The effect of pH on the RhB adsorbed on the spherical activated carbon

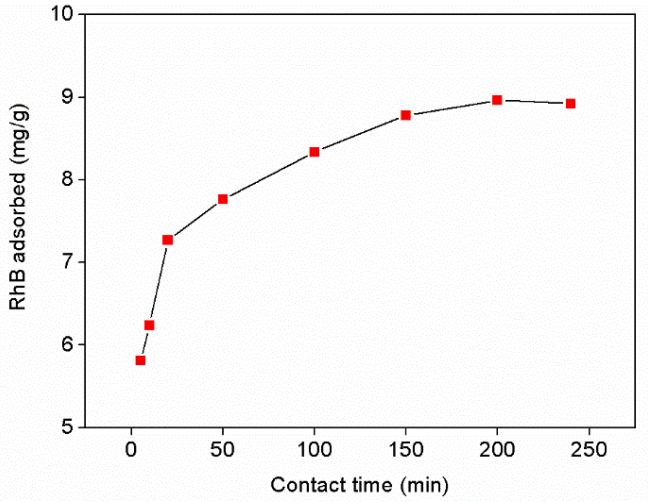

Figure 4. The contact time of RhB adsorbed on the activated spherical carbon

Adsorption Kinetics

The kinetic parameters are very useful for estimating the adsorption rate and providing adsorption process information. The values of the adsorption kinetics parameters are evaluated using the first-order kinetic and second-order kinetic (Wang & Guo, 2020). The equation of the first-order kinetics model is as follows (1):

$$ln\ (q_e - q_t) = ln\ q_e - k_1\ t \qquad (1)$$

where q_t is the amount of RhB which is adsorbed by the adsorbent at time t (mg.g^{-1}) and q_e is the amount of RhB which is adsorbed by the adsorbent in equilibrium conditions (mg.g^{-1}). The first-order kinetics (k_1) rate constant can be obtained by slope by plotting $ln\ (q_e - q_t)$ vs t. The $ln\ (q_e - q_t)$ curve as a function t is a linear curve with a gradient k_1. Based on the obtained data, the curve for the first-order kinetics adsorption of RhB is presented in **Figure 5**. From the linear regression, the value of k_1 (slope) is 0.0194 (min^{-1}) and R^2 is 0.9421. The value of q_e can be obtained through calculations on the intercept resulting in 3.9075 mg g^{-1}.

The second-order kinetics model was also evaluated using equation (2) (Wang & Guo, 2020):

$$\frac{t}{q_t} = \frac{1}{k_2 q_e^{\ 2}} + \frac{1}{q_e} t \qquad (2)$$

where q_e is the amount of RhB absorbed in equilibrium conditions (mg g^{-1}), q_t is the amount of RhB which is adsorbed by the activated carbon at time t (mg g^{-1}). The rate order of second-order kinetics (k_2) can be obtained by calculating the intercept by plotting t/q_t vs t to obtain a linear regression equation. Based on the research data, the second-order adsorption of the RhB kinetic model is presented in **Figure 6**. Based on the linear regression, the value of k_2 is 0.0251 g mg^{-1} min^{-1} calculated from the intercept, with R2=0.9989. The q_e value can be obtained through the calculation on the slope, resulting in 9.0579 mg g^{-1}. The second-order kinetics constant is used to calculate the initial sorption rate (h) using the following equation (3) (Gad & El-Sayed, 2009):

$$h = k_2 q_e^2 \qquad (3)$$

Therefore, the initial sorption rate is 0.2281 mg g^{-1} min^{-1}.

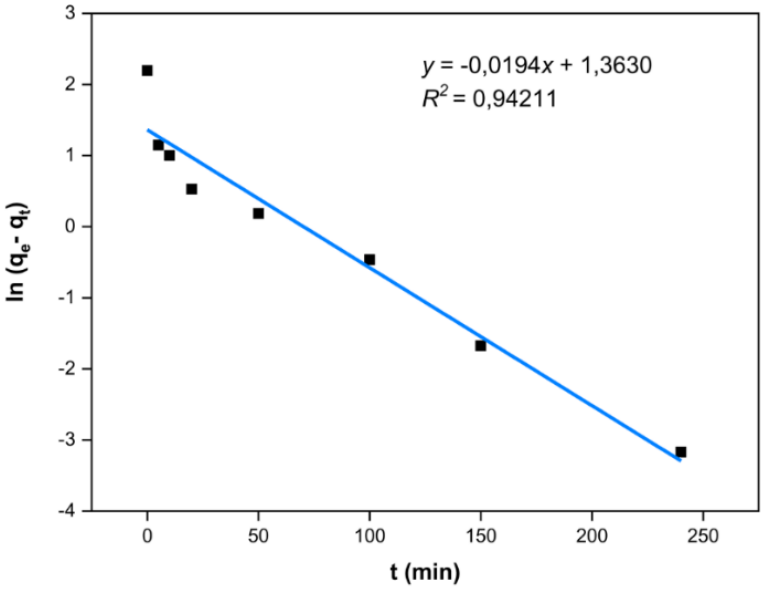

Figure 5. Linear regression curve of the first-order kinetic adsorption of RhB

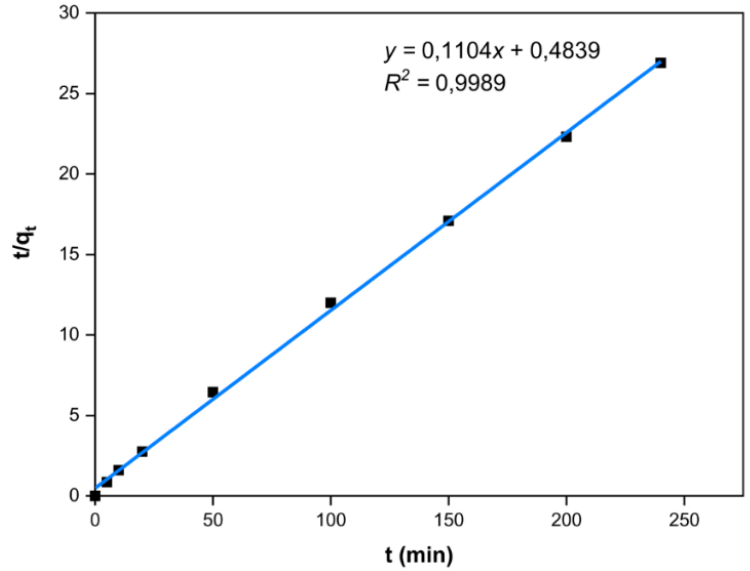

Figure 6. Linear regression curve of the second-order kinetic adsorption of RhB

Table 1 Adsorption kinetics of RhB on the spherical activated carbon

First-order kinetics			Second order kinetics			
q_e (mg g^{-1})	k_1 (min^{-1})	R^2	q_e (mg g^{-1})	k_2 (g $mg^{-1}min^{-1}$)	h (mg $g^{-1}min^{-1}$)	R^2
3.9075	0.0194	0.9421	9.0579	0.0251	0.228	0.9989

The results of first and second-order kinetics of RhB adsorption on spherical carbon were summered in **Table 1**. The adsorption kinetic highly fits with this second-order kinetics (R^2=0.9982). These results are suggesting that the adsorption process was influenced by two variables of adsorbent and adsorbate. Due to the ionic phase, RhB might affect the rate of adsorption kinetics.

Adsorption Isotherms

The essence of understanding the specific relation between the adsorbates and their adsorption on the solid phase at a certain temperature is the adsorption isotherm model (Yaneva et al., 2013). Using the adsorption isotherms, it is possible to evaluate the adsorption process and estimate the maximum capacity of an adsorbent. The common isotherm models used to study solid-liquid adsorption are Langmuir, Freundlich, Temkin, and Elovich.

Determination of adsorption isotherm is carried out by interacting the spherical activated carbon with RhB in an initial concentration of 20-400 mg L^{-1} at 26°C, optimum pH and contact time. The correlation

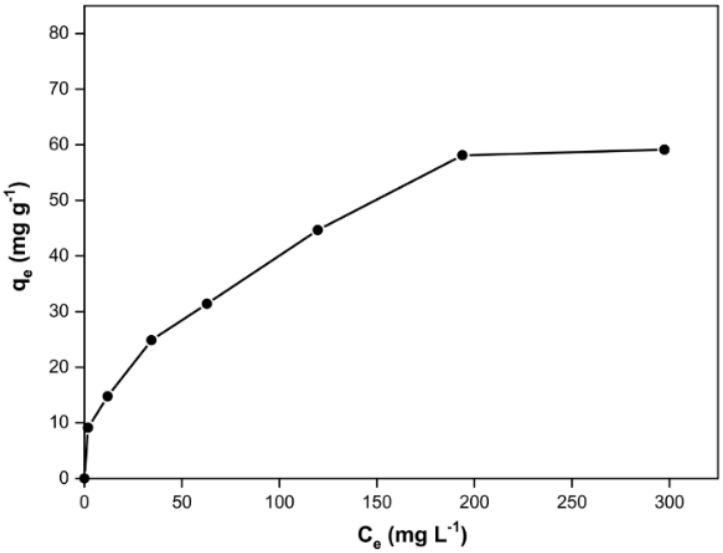

Figure 7. The correlation of the equilibrium RhB concentration (C_e) to adsorbed RhB on spherical activated carbon (q_e)

between the equilibrium RhB concentration (C_e) and the adsorbed mass (q_e) is presented in **Figure 7**. The curve shows that RhB adsorbed increases with increasing concentration of RhB solution until the equilibrium is achieved. The initial concentration of RhB can affect the adsorption process. The higher the concentration, the more RhB adsorbed on the adsorbent until the equilibrium was achieved. The higher the concentration of RhB, the more the particles of the RhB collide with the adsorbent. The equilibrium achieved indicates that adsorption capacity has reached a maximum. These data are used to evaluate the model of adsorption such as Langmuir, Freundlich, Temkin, and Elovich.

The Langmuir isotherm model is associated with the assumption that adsorption occurs in solids that have a homogeneous surface. The absorbed molecule forms one layer (monolayer) on the active side of solids both physically at low temperatures and chemically at higher temperatures (Foo & Hamee, 2010). The adsorption also has a reversible and limited nature. With this assumption, the maximum adsorbate can be calculated using the Langmuir equation as follows:

$$\frac{C_e}{q_e} = \frac{1}{q_m k_L} + \frac{1}{q_m} C_e \qquad (4)$$

where q_e is the amount of RhB adsorbed (mg g^{-1}) at equilibrium concentration (C_e) (mg L^{-1}). There are two important parameters in the Langmuir adsorption isotherm, namely the maximum adsorption capacity (q_m) and the Langmuir constant (k_L) related to the strength of adsorption. These parameters are obtained by plotting data C_e vs C_e/q_e as a linear function. The result of the Langmuir adsorption isotherm is presented in **Figure 8a**. Based on linear regression analysis, the value of 0.9486, 64,516 mg g^{-1} and 0,0296 L mg^{-1} were obtained for R^2, q_m, and k_L, respectively.

The Freundlich adsorption isotherm model represents the relationship between liquid and solid phase equilibrium. This mechanism is based on multilayer adsorption on heterogeneous surfaces. The Freundlich isotherm model is a development of the Langmuir model where Freundlich assumes that in the adsorption process, interactions between adsorbate molecules occur to form an accumulation of layers. The surface of the solid is also heterogeneous where the adsorption site is distributed exponentially. The Freundlich adsorption can be represented by the following equation:

$$ln\ q_e = \frac{1}{n} ln\ C_e + ln\ k_f \qquad (5)$$

where k_f is the Freundlich constant (mg g^{-1}) and $1/n$ is the parameters related to the adsorption intensity which depends on adsorbent heterogeneity. This value is obtained by plotting ln q_e vs ln C_e. Figure 8b shows a linear regression curve of Freundlich's isotherm which shows the R^2 value of 0.8316. The values of $1/n$ and k_f can be found from the calculation of the slope and intercept, 0.593 and 2.642 mg g^{-1}, respectively. It is reported that the value range of $1/n$ is 0−1, when the value approaches 0, the surface heterogeneity of the activated carbon increases (Patrulea et al., 2013). Based on the results, the value of $1/n$ is away from 0, indicating that the adsorption is more homogeneous.

The Temkin isotherm model was also evaluated in this experiment. The heat of adsorption decreases linearly with the increasing number of interactions (Saleh et al., 2017). The equation of Temkin isotherm can be formulated as follow (6):

$$q_e = \frac{RT}{b} ln\ k_T + \frac{RT}{b} ln\ C_e \qquad (6)$$

where B = RT/b is the equation constant associated with heat adsorption (J mol^{-1}), b is the Temkin constant, R is a gas constant (8.314 J mol^{-1} K^{-1}), T is the temperature (K), and k_T is the bond constant in equilibrium conditions related to the maximum bond energy (L g^{-1}). Values B, b, and k_T are obtained by plotting q_e vs ln C_e. The linear curve of the Temkin isotherm is presented in **Figure 8c**. Based on the regression analysis of Temkin's linear isotherm adsorption, the R^2 value was obtained at 0.9000. The values of B, b, and k_T can be calculated from the slope and the intercept that exhibited 10,035 J mol^{-1}, 247.72, and 0,7398 L g^{-1}, respectively.

The next analysis of the adsorption isotherm model is the Elovich isotherm. The adsorption is based on the assumption that the adsorption site increases exponentially to the maximum state. The Elovich adsorption isotherm model shows a multilayer adsorption mechanism on the surface of activated carbon (Saadi et al., 2015). The thermal adsorption model is represented by the following equation (7):

$$ln\frac{q_e}{C_e} = ln\,(K_E q_m) - \frac{1}{q_m} q_e$$

q_m is the maximum adsorption capacity (mgg^{-1}) and K_E is the Elovich constant (Lmg^{-1}). The values of K_E and q_m can be found by plotting the values $ln\ (q_e/C_e)$ vs q_e. The linear curve of the Elovich adsorption isotherm is presented in **Figure 8d**. Based on the linear regression analysis of Elovich isotherm, the q_m value obtained from the calculation of slope is 20.492 mg g^{-1} and the value of K_E is 0.1713 L mg^{-1} from the intercept calculation. The degree of suitability of the Elovic isotherm (R^2) is 0.7986.

The results of Langmuir, Freundlich, Temkin and Elovich's adsorption isotherms are presented in **Table 2**. Based on the comparison of R^2 values, it can be concluded that the adsorption isotherm model which has the best degree of suitability is Langmuir.

Table 2 The calculation isotherm adsorption of Langmuir, Freundlich, Temkin, and Elovich model

Langmuir		Freundlich		Temkin		Elovich	
q_m (mg/g)	64.516	*1/n*	0.593	*B* (J/mole)	10.035	q_m (mg/g)	20.492
k_L (L/g)	0.0296	k_f (mg/g)	2.642	k_T (L/mg)	0.7398	k_E (L/mg)	0.1713
R^2	0.9486	R^2	0.8316	R^2	0.9000	R^2	0.7986

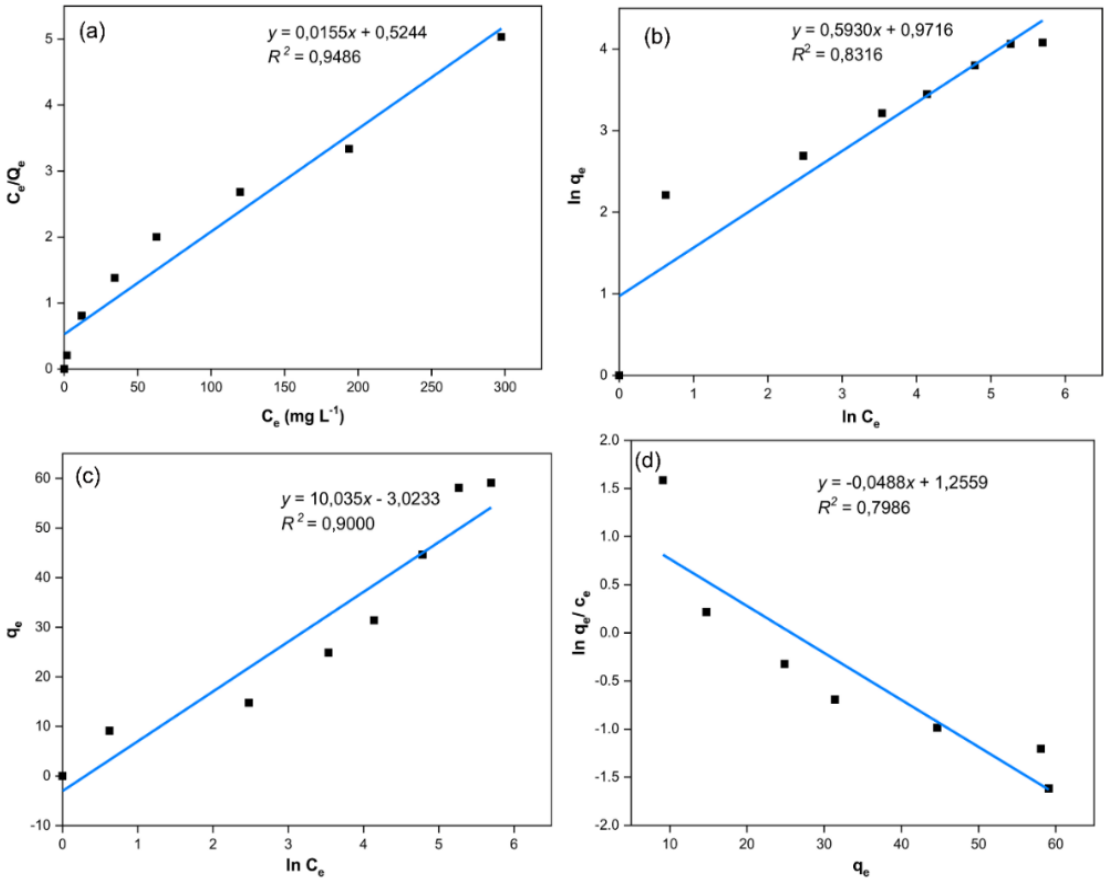

Figure 8. Linear regression of the isotherm adsorption of Langmuir (**a**), Freundlich (**b**), Temkin (**c**) and Elovich (**d**) model.

CONCLUSIONS

Spherical carbon of 3-7 μm in diameter can be synthesized from the waste bagasse liquid using the hydrothermal method. Hydrothermal induces the hydrolysis reaction leading to dehydration, nucleation and spherical formation. The material has been successfully activated using the KOH solution. The spherical activated carbon has an adsorption capacity of 64.52 mg g^{-1} with the optimum adsorption achieved in pH 2, and a contact time of 200 min. The adsorption follows the second-order kinetic and Langmuir isotherm model.

ACKNOWLEDGMENTS

This research was partially supported by the Directorate of Research and Community Services, Ministry of Research, Technology and Higher Education of the Republic of Indonesia (059/SP2H/ LT/DRPM/2018).

REFERENCES

Aljeboree, A. M., Alshirifi, A. N., & Alkaim, A. F. (2017). Kinetics and equilibrium study for the adsorption of textile dyes on coconut shell-activated carbon. *Arabian Journal of Chemistry*, *10*, S3381–S3393.

Amorós-Pérez, A., Cano-Casanova, L., Ouzzine, M., Rufete-Beneite, M., Romero-Anaya, A. J., Lillo-Ródenas, M. A., & Linares-Solano, Á. (2018). Spherical activated carbons with high mechanical strength are directly prepared from selected spherical seeds. *Materials*, *11*, 770.

Arneli, Safitri, Z. F., Pangestika, A. W., Fauziah, F., Wahyuningrum, V. N., & Astuti, Y. (2017). The influence of activating agents on the performance of rice husk-based carbon for sodium lauryl sulfate and chrome (Cr) metal adsorptions. In *IOP Conference Series: Materials Science and Engineering*, *172*, 012007. IOP Publishing.

Arnelli, Aditama, W. P., Fikriani, Z., & Astuti, Y. (2018). Adsorption kinetics of surfactants on activated carbon. In *IOP Conference Series: Materials Science and Engineering*, *349*, 012001. IOP Publishing.

Bedin, K. C., Cazetta, A. L., Souza, I. P. A. F., Pezoti, O., Souza, L. S., Souza, P. S. C., Yokoyama, J. T. C., & Almeida, V. C. (2018). Porosity enhancement of spherical activated carbon: Influence and optimization of hydrothermal synthesis conditions using response surface methodology. *Journal of Environmental Chemical Engineering*, *6*, 991–999.

Beltrame, K. K., Cazetta, A. L., Souza, P. S. C., Spessato, L., Silva, T. L., & Almeida, V. C. (2018). Adsorption of caffeine on mesoporous activated carbon fibers prepared from pineapple plant leaves. *Ecotoxicology and Environmental Safety*, *147*, 64–71.

Chai, L., Huang, Q., Cheng, H., Wang, X., Zhang, L., Li, T. T., Hu, Y., Qian, J., & Huang, S. (2020). Bottom-up preparation of hierarchically porous MOF-modified carbon sphere derivatives for efficient oxygen reduction. *Nanoscale*, *12*, 8785–8792.

Danish, M., Ahmad, T., Hashim, Said, R. N., Akhtar, M. N., Mohamad-Saleh, J., & Sulaiman, O. (2018). Comparison of surface properties of wood biomass activated carbons and their application against Rhodamine B and methylene blue dye. *Surfaces and Interfaces*, *11*, 1–13.

Ding, L., Zou, B., Gao, W., Liu, Q., Wang, Z., Guo, Y., Wang, X., & Liu, Y. (2014). Adsorption of Rhodamine B from aqueous solution using treated rice husk-based activated carbon. *Colloids and Surfaces A*, *446*, 1–7.

Fikri, E., & Veronica, A. (2018). Effectiveness of carbon monoxide concentration reduction on active carbon contact system in burning polystyrene foam. *Journal of Ecological Engineering*, *19*(4), 1–6.

Foo, K. Y., & Hamee, B. H. (2010). Insight into the modeling of adsorption isotherm systems. *Chemical Engineering Journal*, *156*, 2–10.

Gad, H. M. H., & El-Sayed, A. A. (2009). Activated carbon from agricultural by-products for the removal of Rhodamine B from aqueous solution. *Journal of Hazardous Materials*, *168*, 1070–1081.

Guo, J., & Lua, A. C. (2002). Textural and chemical characterizations of adsorbent prepared from palm shell by potassium hydroxide impregnation at different stages. *Journal of Colloid and Interface Science*, *254*, 227–233.

Harihastuti, N., Purwanto, P., & Istadi, I. (2015). Separation of H_2S and NH_3 gases from tofu waste water-based biogas using activated carbon adsorption. In *AIP Conference Proceedings*, *1699*, 060012. AIP Publishing.

Harihastuti, N., Purwanto, P., & Istadi, I. (2017). Carbon dioxide (CO_2) reduction of tofu industrial waste water-based biogas by an integrated process of activated carbon and zeolite adsorption to enhance pipeline quality gas. *Advanced Science Letters*, *23*(6), 5704–5708.

Inyinbor, A. A., Adekola, F. A., & Olatunji, G. A. (2015). Adsorption of Rhodamine B dye from aqueous solution on Irvingia gabonensis biomass: kinetics and thermodynamics studies. *South African Journal of Chemistry*, *68*, 115–125.

Isahak, W. N. R. W., Hisham, M. W. M., & Yarmo, M. A. (2013). Highly porous carbon materials from biomass by chemical and carbonization method: A comparison study.

Journal of Chemistry, *2013*, 620346.

Li, C., Ni, W., Zang, X., Wang, H., Zhou, Y., Yang, Z., & Yan, Y. (2020). Magnesium oxide anchored into a hollow carbon sphere realizes synergistic adsorption and activation of CO_2 for electrochemical reduction. *Chemical Communications*, *56*, 6062–6065.

Li, M., Li, W., & Liu, S. (2011). Hydrothermal synthesis, characterization, and KOH activation of carbon sphere from glucose. *Carbohydrate Research*, *346*, 999–1004.

Liu, Z., Sun, Y., Xu, X., Qu, J., & Qu, B. (2020). Adsorption of Hg(II) in an aqueous solution by activated carbon prepared from rice husk using KOH activation. *ACS Omega*, *5*(45), 29231–29242.

Li, Y., Li, D., Zhao, X., & Wu, M. (2016). Superior CO_2, CH_4, & H_2 uptakes over ultrahigh-surface-area carbon spheres prepared from sustainable biomass-derived char by CO_2 activation. *Carbon*, *105*, 454–462.

Lua, A. C., & Yang, T. (2004). Effect of activation temperature on the textural and chemical properties of potassium hydroxide activated carbon prepared from a pistachio-nut shell. *Journal of Colloid and Interface Science*, *274*, 594–601.

Patrulea, V., Negrulescu, A., Mincea, M. M., Pitulice, L. D., Spiridon, O. B., & Ostafe, V. (2013). Optimization of the removal of copper (II) ions from aqueous solution on chitosan and cross-linked chitosan beads. *BioResources*, *8*, 1147–1165.

Qi, Y., Zhang, M., Qi, L., & Yang, Q. (2016). The mechanism for formation and growth of carbonaceous spheres from sucrose by hydrothermal carbonization. *RSC Advances*, *6*, 20814–20823.

Rouquerol, F., Rouquerol, J., Sing, K. S. W., Llewellyn, P., & Maurin, G. (2014). *Adsorption by powders and porous solids, principles, methodology, and applications*. London: Academic Press.

Ruhmawati, T., Budiansyah, T., & Fikri, E. (2019). Reducing the ammonia content of hospital liquid waste by active carbon plastic ore adsorption. *International Journal of Environment and Waste Management*, *25*(1), 121–129.

Saadi, R., Saadi, Z., Fazaeli, R., & Fard, N. E. (2015). Monolayer and multilayer adsorption isotherm models for sorption from aqueous media. *Korean Journal of Chemical Engineering*, *32*, 787–799.

Saleh, T. A., Sari, A., & Tuzen, M. (2017). Optimization of parameters with experimental design for the adsorption of mercury using polyethyleneimine modified-activated carbon. *Journal of Environmental Chemical Engineering*, *5*, 1079–1088.

Sevilla, M., & Antonio, B. F. (2009). Chemical and structural properties of carbonaceous products obtained by hydrothermal carbonization of saccharides. *Chemistry-A European Journal*, *15*, 4195–4203.

Sun, S., Cao, J., Xu, Z., Yang, Z., Xiong, W., Song, P., Zhong, R., & Peng, S. (2020). KOH activated ZIF-L derived N-doped porous carbon with enhanced adsorption performance towards antibiotics removal from aqueous solution. *Journal of Solid State Chemistry*, *289*, 121492.

Tagliavini, M., Engel, F., Weidler, P. G., Scherer, T., & Schafer, A. I. (2017). Adsorption of estrogenic micropollutants on polymer-based spherical activated carbon (PBSAC). *Journal of Hazardous Materials*, *337*, 126–137.

Wang, F., Zhang, Y., Fang, Q., Li, Z., Lai, Y., & Yang, H. (2021). Prepared PANI@nano hollow carbon sphere adsorbents with lappaceum shell-like structure for high-efficiency removal of hexavalent chromium. *Chemosphere*, *263*, 128109.

Wang, J., & Guo, X. (2020). Adsorption kinetic models: Physical meanings, applications, and solving methods. *Journal of Hazardous Materials*, *390*, 122156.

Wang, X., Xin, C., Shi, C., Dong, A., & Wang, K. (2018). Simple preparation of spherical activated carbon with mesoporous structure from phenolic resol and associated catalytic performance in isobutane dehydrogenation. *Transactions of Tianjin University, 24*, 351–360.

Xu, T., Ji, H., Gu, Y., Tong, T., Xi, Y., Zhang, L., & Zhao, D. (2020). Enhanced adsorption and photocatalytic degradation of perfluorooctanoic acid in water using iron (hydr)oxides/carbon sphere composite. *Chemical Engineering Journal*, *388*, 124230.

Yaneva, Z. L., Koumanova, B. K., & Georgieva, N. V. (2013). Linear and non-linear regression methods for equilibrium modeling of p-nitrophenol biosorption by Rhizopus oryzae: comparison on error analysis criteria. *Journal of Chemistry*, *2013*, 517631.

Yaumi, A. L., Bakar, M. Z. A., & Hameed, B. H. (2018). Melamine-nitrogenated mesoporous activated carbon derived from rice husk for carbon dioxide adsorption in fixed-bed. *Energy,* 155, 46–55.

Zhu, X., Liu, Y., Zhou, C., Zhang, S., & Chen, J. (2014). Novel and high-performance magnetic carbon composite prepared from waste hydrochar for dye removal. *ACS Sustainable Chemistry & Engineering*, *2*, 969–977.